NOTES AND CORRESPONDENCE

A Simple Kinematic Mechanism for Mixing Fluid Parcels across a Meandering Jet*

AMY S. BOWER

Woods Hole Oceanographic Institution, Woods Hole, Massachusetts

13 November 1989 and 16 July 1990

ABSTRACT

Recent observations of fluid parcel pathways in the Gulf Stream using isopycnal RAFOS floats revealed a striking pattern of cross-stream and vertical motion associated with meanders (Bower and Rossby 1989). In an attempt to explain the observed pattern, a two-dimensional kinematic model of a meandering jet has been developed which enables examination of the relationship between streamfunction patterns and fluid parcel trajectories. The streamfunction fields are displayed in a reference frame moving with the wave pattern so motions of fluid parcels *relative* to the jet can be seen more easily.

The results suggest that the observed pattern of cross-stream motion results primarily from the downstream phase propagation of meanders. The model successfully reproduces several of the most distinctive features of the float observations: 1) entrainment of fluid into the Gulf Stream occurs at the leading edges of meander extrema while detrainment takes place at the trailing edges; 2) exchange between the Gulf Stream and its surroundings increases with a) increasing depth, b) increasing meander amplitude, and c) increasing wave phase speed.

Transport calculations from the model streamfunction fields indicate that for typical phase speeds (10 km d^{-1}) and amplitudes (50 km), roughly 90% of the fluid in the surface layers of the Gulf Stream flows downstream in the jet while 10% continuously recirculates into the surroundings. In the deep main thermocline, where downstream speeds are less, only about 40% of the fluid is retained in the jet and 60% is trapped in the recirculating cells. It is concluded that this simple kinematic mechanism could lead to cross-stream mixing of fluid parcels, especially in the deeper layers of the Gulf Stream.

1. Introduction

Recent observations of fluid parcel pathways in the Gulf Stream have revealed a striking pattern of vertical and cross-stream motion, which is closely linked to the meandering of the jet (Bower and Rossby 1989; hereafter, BR). Using the trajectories of 37 constant-density RAFOS floats launched in the center of the stream near Cape Hatteras, BR documented a pattern of upward and onshore (downward and offshore) motion between meander troughs and crests (crests and troughs) (Fig. 1). The cross-stream excursions were also apparent in the speed records along the float trajectories, which showed a maximum in downstream speed when the floats were near the center of the Gulf Stream (cross-stream position determined from float's temperature and pressure) and decreased as the floats moved away from the center.

Cross-stream displacements away from the jet axis on the order of ±20 km were commonly observed as the floats traveled between meander extrema (compared to the 100 km nominal width of the jet), and in many cases, floats were seen to cross out of the current altogether (see BR Figs. 10 and 11 for examples). Based on a comparison of all the trajectories in the main thermocline, BR came to the following conclusions concerning fluid exchange between the Gulf Stream and the surrounding fluid: 1) fluid from the center of the stream is most often lost from the current at the trailing edges of meander troughs and crests, while entrainment takes place primarily at the leading edges of meander crests (Fig. 2); 2) exchange occurs much more readily in the lower main thermocline than in the upper layers (Fig. 3); and 3) cross-stream motions and entrainment and detrainment of fluid are enhanced when the curvature of the Gulf Stream path is very large (Fig. 4). Shaw and Rossby (1984) and Owens (1984) have also noted the increase in exchange with depth based on the trajectories of SOFAR floats.

The purpose of this work is to describe a simple kinematic mechanism for fluid exchange in the Gulf Stream region which appears to reproduce many of the Lagrangian observations without invoking any complex dynamical processes. A simple two-dimensional model of a meandering jet has been developed, and trajectories of fluid parcels *relative* to the wave pattern are determined by examining the streamfunction field in a reference frame moving at the wave propagation speed. This technique has been used previously by Regier and Stommel (1979) and Flierl (1981) to examine

* Contribution No. 7245 from the Woods Hole Oceanographic Institution.

Corresponding author address: Dr. Amy Bower, Clark 315, Woods Hole Oceanographic Institution, Woods Hole, MA 02543.

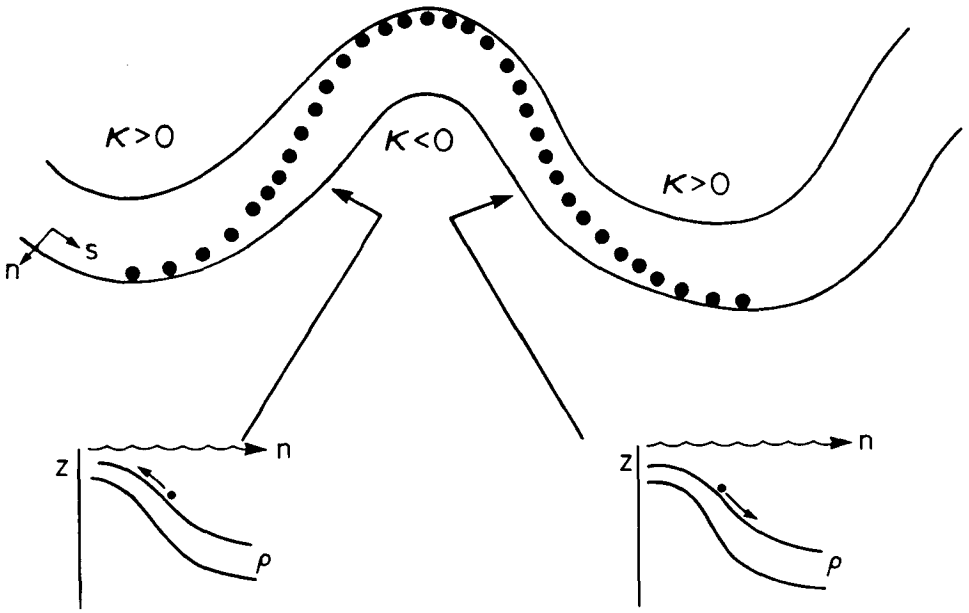

FIG. 1. Schematic view of three-dimensional motion of RAFOS floats. Dots indicate trajectory of a float through a Gulf Stream meander (from Bower and Rossby 1989).

fluid parcel trajectories in a variety of kinematic flow regimes. Although many of their results are generally applicable to the Gulf Stream flow field, this work focuses on 1) the features specific to the Gulf Stream, such as cross-stream structure of the jet and its baroclinicity, which affect fluid parcel motion, and 2) comparison with recently acquired RAFOS float observations.

Owens (1984) briefly examined the kinematics of fluid parcels in the Gulf Stream but only considered the case for small-amplitude meanders. He concluded that fluid parcels with downstream speeds exceeding the phase speed (c) of the meanders would be trapped in the current, while those with a speed less than c would be "left behind" and would not be trapped. For example, given a phase speed of 10 cm s^{-1}, typical for meanders east of 70°W (Gilman 1988), this implies that all fluid parcels with a downstream speed greater than 10 cm s^{-1} would remain trapped in the current. In fact, the RAFOS float observations show that even fluid parcels in the center of the Gulf Stream with downstream speeds of 100 cm s^{-1} can work their way to the edges and escape. This phenomenon will be shown to be the result of the finite (and often large) amplitude of the meanders.

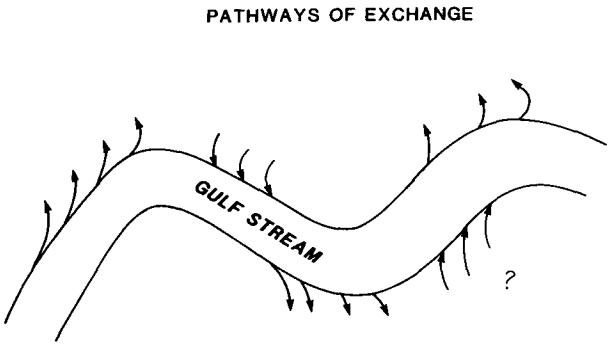

FIG. 2. Schematic diagram showing regions of fluid exchange between the Gulf Stream and its surroundings based on the trajectories of RAFOS floats (from Bower and Rossby 1989).

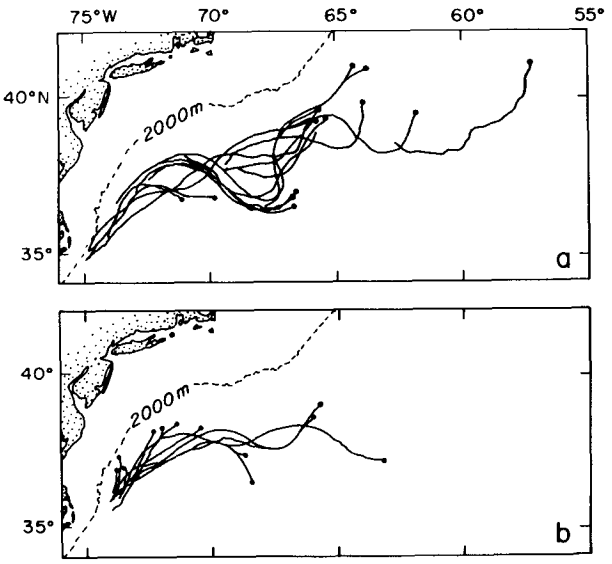

FIG. 3. (a) Trajectories of RAFOS floats on temperature surfaces between 11° and 16°C up to the point of first escape; (b) same as for (a) but for floats on temperature surfaces between 7° and 11°C (from Bower and Rossby 1989). Note how floats in (b) appear to escape from the stream much more quickly.

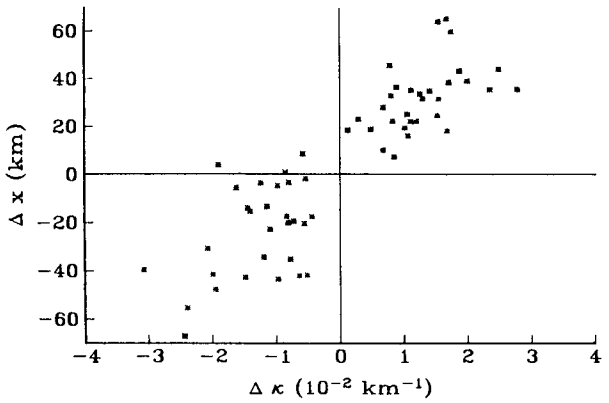

FIG. 4. Cross-stream displacement of RAFOS floats in meanders as function of change in trajectory curvature (from Bower and Rossby 1989).

Meteorologists have also studied the relationship between streamfunction patterns and air parcel trajectories (Rossby 1942; Palmen and Newton 1969, section 8.2). If one carefully examines the inferred trajectories of air parcels in the propagating waves of the jet stream, one finds that the motions of air parcels relative to the jet stream axis are very similar to what has been observed with the RAFOS floats (see Palmen and Newton, Fig. 8.8). In this work it is shown that the mechanism responsible for the motion of air parcels relative to the jet stream axis is applicable to the Gulf Stream as well.

In the next section, the basic principle by which fluid parcels move relative to the Gulf Stream axis is reviewed briefly, and the kinematic model is described. In section 3, the model trajectories of fluid parcels relative to the wave pattern are presented. The effects of varying three different parameters are examined: 1) magnitude of downstream speed at the jet axis (this variation simulates the conditions at different depths in the Gulf Stream), 2) phase speed of the meanders, and 3) meander amplitude. In section 4 the relevance of these results to water property distributions in the Gulf Stream region is discussed.

2. Methodology

The relationship between trajectories and propagating streamfunction patterns is discussed in depth by several authors (Flierl 1981; Regier and Stommel 1979; Palmen and Newton 1969). The principles are described only briefly here to emphasize specific features of the Gulf Stream flow region.

Consider the two-dimensional flow field in the x–y plane shown in Fig. 5 (x positive eastward, y positive northward). The streamfunction pattern is propagating to the east at phase speed c in this case, and the velocity field has a jet-like structure as shown. The velocity at any point is given by

$$\mathbf{V}(x, y, t) = u(x, y, t)\mathbf{i} + v(x, y, t)\mathbf{j}$$

where

$$u = -\partial\Psi/\partial y \quad \text{and} \quad v = \partial\Psi/\partial x.$$

The motion of a fluid parcel *relative* to the wave pattern, however, is given by

$$\mathbf{V}\,\text{rel} = (u - c)\mathbf{i} + v\mathbf{j},$$

and is shown in the figure for the case where $u > c > 0$ (the usual situation in the upper Gulf Stream). While flowing downstream, it is apparent that the fluid parcel moves to the left of the jet axis (looking downstream) into a region of weaker downstream speed. At this point, the velocity vector relative to the wave pattern will veer even more northerly and the fluid parcel will continue to move away from the jet axis (until it reaches the meander crest, at which point v changes sign and the parcel begins to move back toward the jet axis). If on its traverse from meander trough to crest, the parcel reaches a point where $u < c$, the wave crest will be moving eastward faster than the fluid parcel. At this point, the parcel will not continue downstream in the jet until the next crest overtakes it.

RAFOS floats traveling from trough to crest almost always crossed the jet in a similar manner (from right to left, facing downstream, BR). When floats escaped from the jet during this traverse, it was always to the north and usually just upstream of the crest (Fig. 2). The fact that the RAFOS floats follow density surfaces (which slope steeply across the current) and thus have a significant vertical component of motion, does not pose a problem. Simply consider the two-dimensional plane shown in Fig. 5 to be a density surface. As the fluid parcels move laterally relative to the jet axis, they must also move upward or downward to conserve density. It seems plausible, therefore, that the vertical velocity pattern observed with the RAFOS floats is simply the response of the parcels to the propagation of the

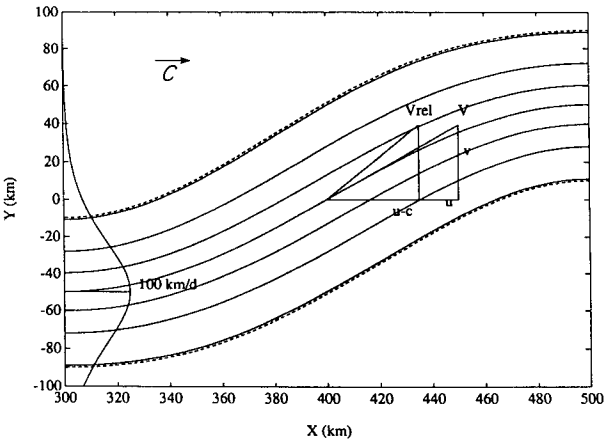

FIG. 5. Streamfunction field, with eastward phase propagation, showing jet structure and velocity vectors in fixed (V) and moving (V rel) reference frames.

wave field. This point will be discussed in more detail later.

In order to examine fluid motion relative to the wave pattern for a variety of flow conditions, a simple two-dimensional streamfunction field has been developed which resembles the flow field in the Gulf Stream. By choosing a kinematic model rather than a dynamical one, the full range of wave amplitudes and phase speeds which are observed in the Gulf Stream can be explored without being restricted to (a) the small-amplitude assumption or (b) the case $u \ll c$ required by linear theory.

The streamfunction has the form:

$$\Psi(x, y, t) = \Psi_0\left\{1 - \tanh\left[\frac{y - y_c}{\lambda/\cos(\alpha)}\right]\right\} \quad (1)$$

where

Ψ_0 scale factor, which with λ, determines maximum downstream speed,
y_c $A\sin[k(x - c_x t)]$, defines center streamline,
A wave amplitude,
k $2\pi/L$, the wave number,
λ 40 km, the scale width of the jet,
α $\tan^{-1}\{Ak\cos[k(x - c_x t)]\}$, direction of current.

The $\cos(\alpha)$ term is included to give the jet uniform width everywhere. Since the flow is not steady, trajectories and streamlines will not coincide. For ease of presentation, it is convenient to transform the streamfunction field into a reference frame moving with the phase speed, c_x. In the moving frame, the streamfunction has the form:

$$\Psi'(x', y') = \Psi_0\left\{1 - \tanh\left[\frac{y' - y'_c}{\lambda/\cos(\alpha')}\right]\right\} + c_x y', \quad (2)$$

where

$$y'_c = A\sin(kx')$$

$$\alpha' = \tan^{-1}[Ak\cos(kx')].$$

The streamfunction in this frame is independent of time and, thus, streamlines can be interpreted as trajectories of fluid parcels *relative* to the moving wave. Three parameters will be varied to examine their impact on cross-stream motion and fluid exchange: 1) magnitude of downstream speed at the jet center ($s_c = \Psi_0/\lambda$), 2) phase speed (c_x), 3) wave amplitude (A).

3. Results

a) Downstream speed

In Fig. 6, the streamfunction is shown in the reference frame moving with c_x for three different values of s_c, the maximum speed in the center of the jet. The contour interval is 1000 km^2 d^{-1} with low values of Ψ' at the top of each plot (indicating generally eastward flow). Superimposed by the dashed lines are the center

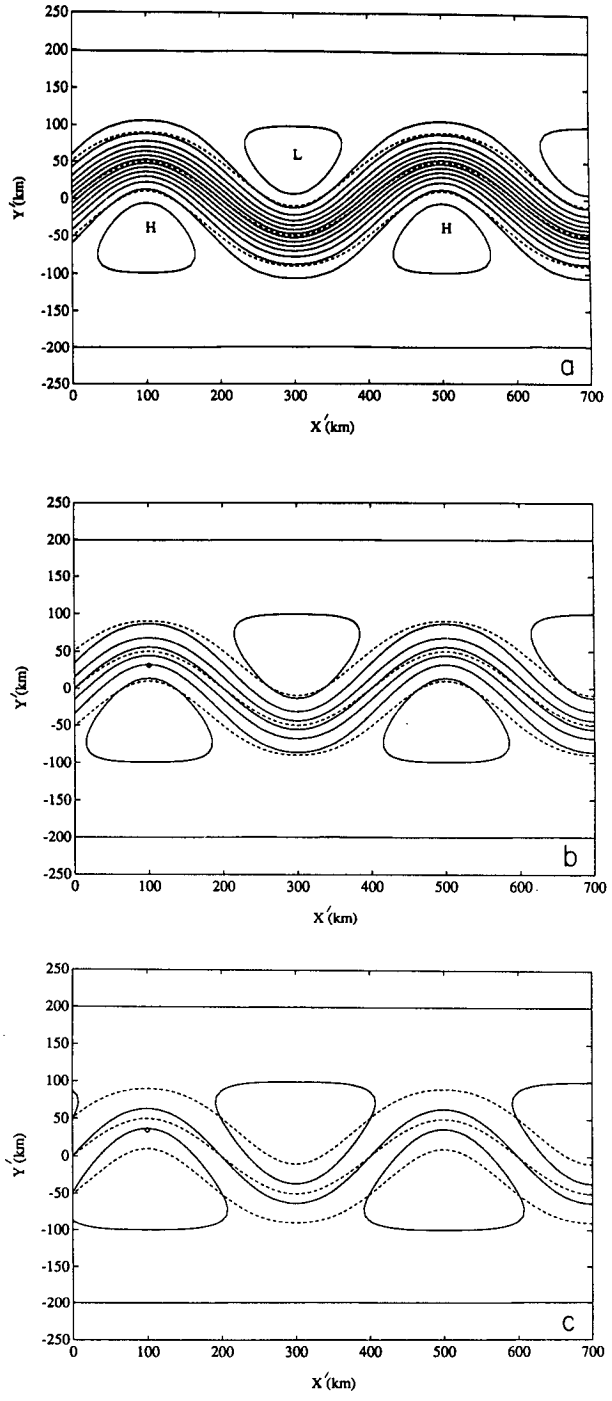

FIG. 6. Streamfunction patterns in a reference frame moving with the wave phase speed, c_x (solid contours). Dashed contours are center streamline and outer edges of jet in fixed frame at $t = 0$. Wave parameters are: $c_x = 10$ km d^{-1}, $A = 50$ km, $L = 400$ km, and $s_c =$ (a) 200 km d^{-1}; (b) 100 km d^{-1}; and (c) 50 km d^{-1}.

streamline and outer edges of the jet (at $\pm\lambda = \pm 40$ km, total width = 80 km) at $t = 0$ in the fixed frame. This allows one to easily see the motion of parcels relative to the jet axis, indicated when the solid and dashed

contours converge or diverge. The values of Ψ_0 have been chosen to give speeds in the center of the jet of (a) 200 km d^{-1} (surface Gulf Stream), (b) 100 km d^{-1} (midthermocline), and (c) 50 km d^{-1} (lower thermocline) (1 km $d^{-1} \approx 1$ cm s^{-1}). These representative speeds have been taken from Halkin and Rossby (1985).

It is evident from Fig. 6a that most of the fluid moves downstream in the jet. Some fluid near the edges is trapped in recirculating cells, represented by the closed contours, which travel downstream with the wave pattern. (In the fixed reference frame, fluid parcels in the recirculating cells will not actually move westward, but will become nearly stationary outside the jet until the next meander crest or trough overtakes them.) There is evidence of some cross-stream motion at this level, especially near the edges, indicated by the crossing of the solid and dashed contours. Note that cross-stream motion near the center of the jet is less due to the higher downstream speeds here.

In Fig. 6b, which represents the density surface closest to that where most of the RAFOS measurements were made, the cross-stream motion of the parcels is more pronounced, especially at the edges. For example, a parcel tagged 20 km south of the jet axis in the first crest (marked with 'O') will be about 35 km south of the axis in the next trough. In addition, the recirculating cells impinge more closely on the jet.

In Fig. 6c, for $s_c = 50$ km d^{-1}, the cross-stream motion is a pronounced feature, even at the jet axis. In addition, the recirculating cells come very close to the axis in the meander extrema. This implies that if a fluid parcel is tagged just 10 km south of the axis in the first crest (again marked with 'O'), its subsequent trajectory will not show it traveling along the jet, but instead will show the parcel escaping from the jet (at least temporarily) and then reentering the jet as the next trough approaches. In all three cases, the regions indicated for entrainment and detrainment correspond well with the float observations (Fig. 2). In addition, the increase in exchange with depth seen in the float data (Fig. 3) is reproduced in the model by the penetration of the recirculating cells into the center of the jet at the deeper levels.

b) Phase speed

In order to examine the effects of variable phase speed and wave amplitude (section 3c) only, s_c has been set to 100 km d^{-1}, a value typical of the midthermocline. Figures 6b and 7a,b show the streamfunction fields for three values of c_x; 10 km d^{-1}, 20 km d^{-1}, and -20 km d^{-1}. Ten kilometers per day is near the average phase speed for meanders east of 73°W as reported by Gilman (1988), whereas 20 km d^{-1} is more typical of meanders closer to Cape Hatteras (Watts and Johns 1982). Sometimes meanders are observed to retrogress, which is represented in this study by Fig. 7b with $c_x = -20$ km d^{-1}.

First comparing Fig. 6b and Fig. 7a, one sees that there are significantly larger cross-stream displacements when the phase speed is doubled. In the fast propagating case, a parcel originally tagged at the jet axis in the first crest ('O') will be displaced about 30 km south of the axis by the time it reaches the next trough. The recirculating cells are more intense and come quite close to the jet axis in the meander extrema. The substantial differences between these two figures clearly illustrates that at increase in phase speed enhances exchange rates.

Figure 7b illustrates the case for retrograde phase propagation ($c < 0$). Here, fluid parcels cross the axis from north to south between troughs and crests and vice versa between crests and troughs. This pattern of motion has occasionally been observed with the RAFOS floats (Bower et al. 1986; T. Rossby, personal communication). An example is shown in Fig. 8. Between yeardays 280 and 283, RAFOS 58 was approaching a meander crest, in which case onshore motion (indicated by vertical motion upward) is usually expected. The pressure record, however, clearly indi-

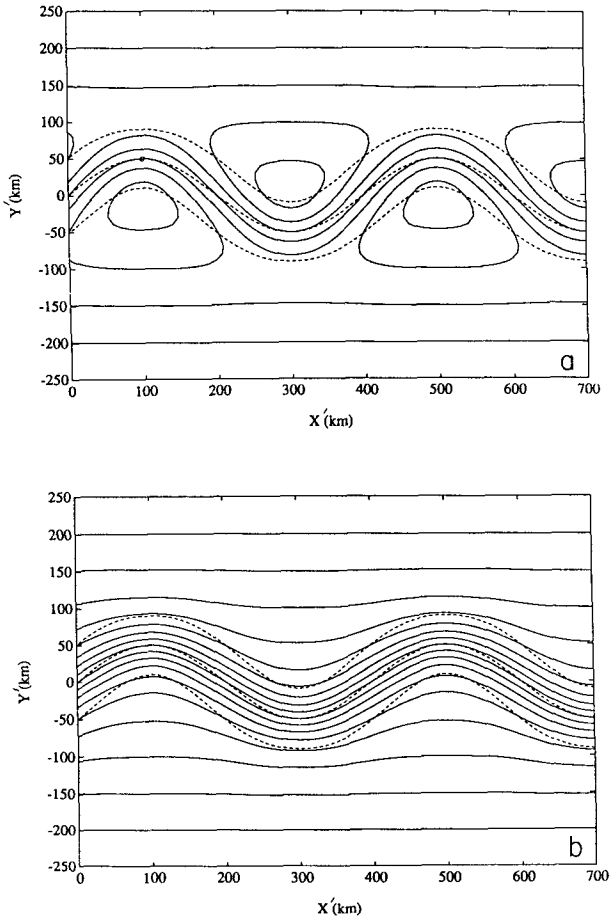

FIG. 7. Same as for Fig. 6 except wave parameters are: $A = 50$ km, $L = 400$ km, $s_c = 100$ km d^{-1}, and c_x = (a) 20 km d^{-1}; (b) -20 km d^{-1}.

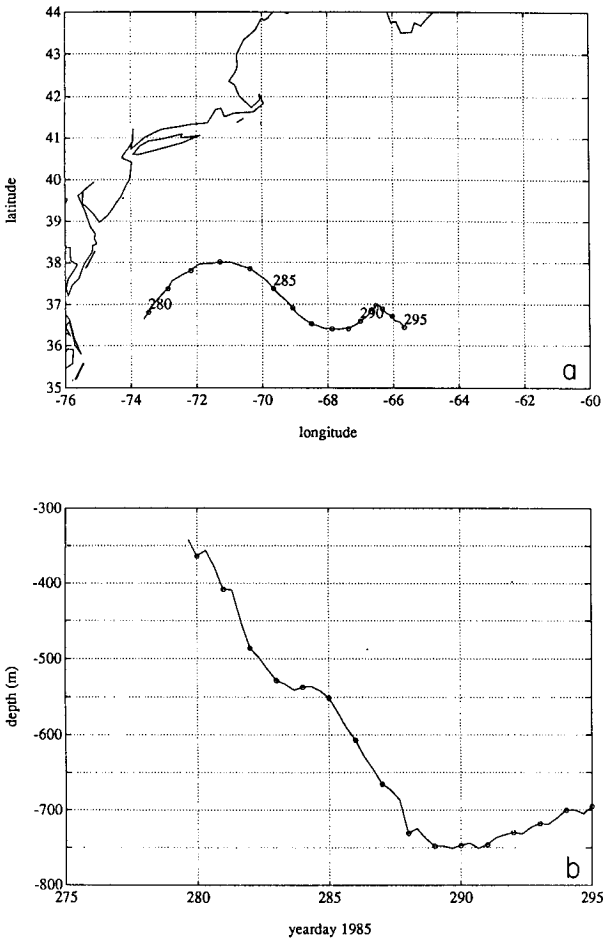

FIG. 8. (a) Trajectory and (b) pressure record for RAFOS 58 launched in 1985. Dots are every 24 hours.

cates downward (offshore) motion during this period. This would indicate that the wave crest was retrogressing to the west (or northwest) rather than the usual eastward propagation. The sequence of satellite images shown by BR Figs. 17a–c for this time period shows, at least crudely, that this meander crest may in fact have been steepening to the northwest.

c) *Wave amplitude*

Finally, in Figs. 6b and 9a,b, the effect of wave amplitude on fluid exchange is examined. Here again the focus is on the midthermocline level. Amplitude-to-wavelength ratios typical of the range observed in the Gulf Stream (Gilman 1988) have been chosen to represent various conditions. At very low amplitude, most of the fluid flows downstream, and there is relatively little cross-stream displacement of parcels (Fig. 9a). This is the case Owens (1984) considered. As the amplitude increases, however (Figs. 6b and 9b), both the cross-stream displacements and the amount of fluid trapped in the recirculating cells increase substantially.

The reason for these increases is apparent if one carefully examines Fig. 5. As the wave amplitude increases, more of the downstream velocity is contained in the v-component and less in the u-component. The fluid parcels are increasingly unable to "keep up" with the wave pattern propagating to the east. Eventually, at very large amplitudes, there is very little fluid progressing downstream in the jet; nearly all the fluid is trapped in the recirculating cells. This result was also observed in the float data. Floats made larger cross-stream excursions when the curvature change between meander extrema was large (Fig. 4), a circumstance usually associated with large-amplitude meanders.

d) *Relative transports in jet and recirculating cells*

These results are summarized more quantitatively in Figs. 10b,c. Shown here is the ratio of transport in the jet to the total transport, including both the jet and the recirculating cells, for a variety of flow conditions found in the Gulf Stream. The total transport is given by the difference in streamfunction between the high

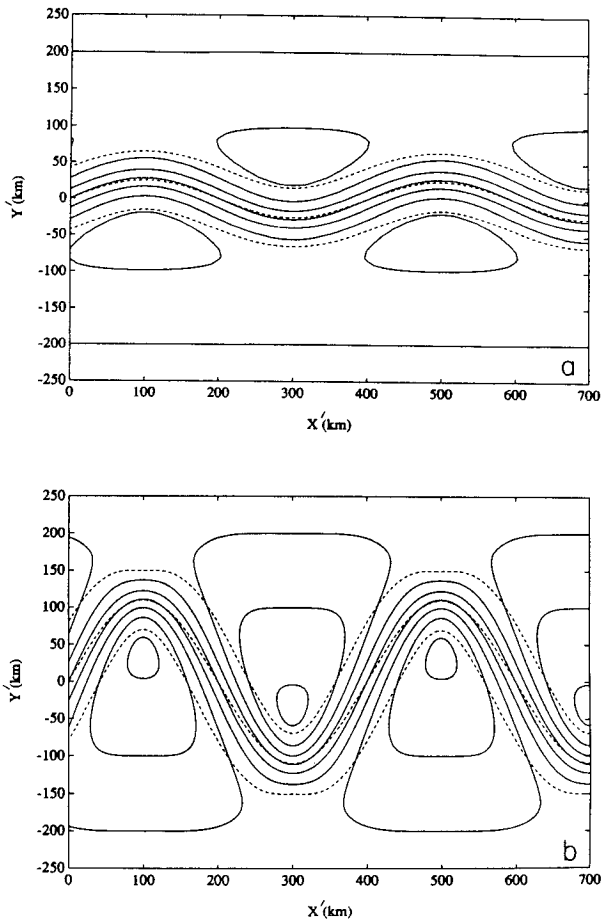

FIG. 9. Same as for Fig. 6 except wave parameters are: c_x = 10 km d^{-1}, L = 400 km, s_c = 100 km d^{-1}, and A = (a) 25 km; (b) 100 km.

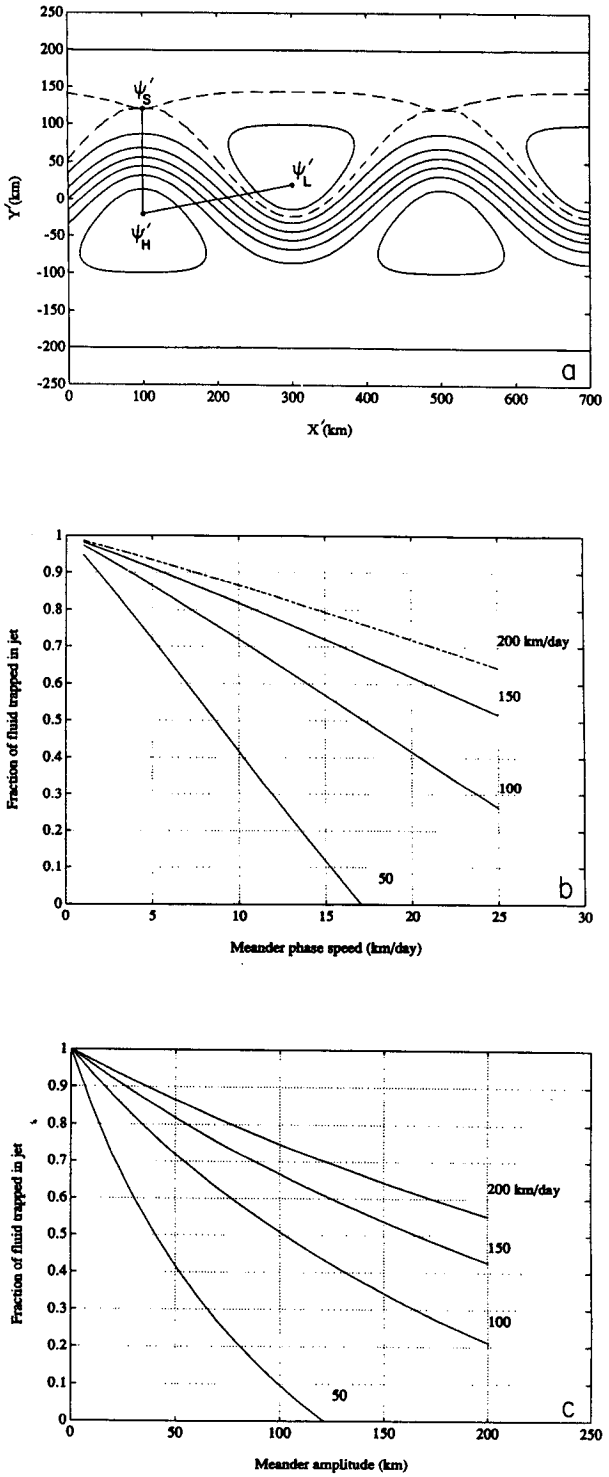

FIG. 10. (a) Same as for Fig. 6b, except figure shows streamline separating jet and recirculating cells (dashed lines), and locations of high center, low center, and stagnation point (see text). Also shown is ratio of transport in jet to total transport of jet and recirculation cells as functions of (b) phase speed (wave amplitude fixed at 50 km) and (c) wave amplitude (phase speed fixed at 10 km d^{-1}), for several values of s_c, the maximum downstream speed in the center of the jet.

and low recirculation cells [$\Psi'(100\text{ km}, y'_H) - \Psi'(300\text{ km}, y'_L) = (\Psi'_H - \Psi'_L)$; Fig. 10a]. This transport is the sum of the jet transport plus the transport in the two cells. The difference between the streamfunction at the center of the high and that at the stagnation point across the jet, [$\Psi'(100\text{ km}, y'_H) - \Psi'(100\text{ km}, y'_S) = (\Psi'_H - \Psi'_S)$], on the other hand, is the sum of the jet transport plus that of *one* cell. From these expressions, the transport of the jet alone is $2(\Psi'_H - \Psi'_S) - (\Psi'_H - \Psi'_L) = \Psi'_H + \Psi'_L - 2\Psi'_S$. The positions of the three critical points (y'_H, y'_L, y'_S) are found by setting $\partial\Psi'/\partial y' = 0$ at $x = 100$ km and $x = 300$ km and solving for y'. The quantity Ψ' at each of these points is then calculated analytically, the total transport and the jet transport are found from the expressions above, and their ratio is evaluated. Note that all transports are calculated in the moving reference frame and ratios reflect the amount of fluid flowing downstream in the jet alone versus the amount trapped in the recirculation cells plus that flowing downstream.

In Fig. 10b, the effect of phase speed is clearly shown, with the percent of fluid flowing downstream decreasing with increasing phase speed at all levels. The effect is more pronounced when the downstream speed is less (e.g., $s_c = 50$ km d^{-1}). For typical $c_x = 10$ km d^{-1}, one can see from the figure that about 87% of the fluid stays in the jet at the level where $s_c = 200$ km d^{-1}, whereas only 42% is retained when $s_c = 50$ km d^{-1}.

The effect of wave amplitude on relative transports is shown in Fig. 10c. As seen in Fig. 9, the amount of fluid carried in the jet decreases with increasing amplitude, and the effect is more pronounced in the deeper layers. Again, for a typical phase speed of 10 km d^{-1} and amplitude of 100 km (amplitude-to-wavelength ratio = 0.25), 75% of the fluid is trapped in the jet at shallow levels ($s_c = 200$ km d^{-1}) versus only 10% for $s_c = 50$ km d^{-1}.

4. Discussion and summary

The streamfunction fields presented here represent an idealized situation, namely a fixed wave pattern propagating steadily in one direction. In reality, the Gulf Stream (and other strong baroclinic jets) exhibits continuously evolving patterns, where downstream speed, wave amplitude, and phase speed all vary, sometimes very rapidly, in space and time. It is fairly easy, however, to extend the results shown here to the time-varying domain, and imagine pathways of exchange alternately opening and closing as the meander pattern evolves. For example, as fluid parcels proceed downstream from Cape Hatteras, meander phase speeds are observed to decrease (Gilman 1988), in which case the fluid parcels would find fewer and fewer pathways of escape. At the same time, however, wave amplitude increases dramatically out to about 60°W, which in turn would tend to open more pathways of exchange. It is quite possible that these two competing

effects tend to compensate for one another with the result that exchange does not increase *substantially* with downstream distance. This idea is supported by the work of Bower et al. (1985), who showed that in the upper layers of the stream, property gradients (of dissolved oxygen in particular) are aligned with the current and are maintained for considerable downstream distances (out to about 50°W).

The significant increase in exchange with depth demonstrated in the model is quite evident in both the float observations and hydrographic data. The results presented here showed that where the downstream speeds are low, but still greater than c_x, the recirculating cells penetrate to the center of the current. Under conditions of significant variations in phase speed or wave amplitude, one can envision a multitude of exchange pathways between the *center* of the jet and the surrounding fluid. The effect of an ensemble of meanders with varying characteristics would be to thoroughly stir the fluid in the deeper layers of the Gulf Stream and to destroy any property gradients which might otherwise be aligned with the current.

Leaman et al. (1989) and Bower et al. (1985) describe the distribution of potential vorticity and other properties along density surfaces in the Gulf Stream region. They show a gradual weakening in the cross-stream gradients with increasing depth such that below about 11°C, the distributions are nearly uniform across the jet. This is about the level where $s_c = 100$ km d^{-1} (Halkin and Rossby 1985) in the canonical stream. These results are consistent with the substantial increase in pathways of exchange with increasing depth shown in the model.

In summary, it appears that the cross-stream motion of fluid parcels, and the increase in fluid exchange with depth in the Gulf Stream can be explained in terms of the relationship between a propagating wave pattern and fluid parcel trajectories. This mechanism does not explain all the complex behavior of fluid parcels in the Gulf Stream; no doubt there are important dynamical processes which also govern their motion. However, the kinematic mechanism appears to adequately account for the broadscale features of fluid motion in the Gulf Stream.

Acknowledgments. The author gratefully acknowledges the following individuals for their contributions to this work: J. Pedlosky and H. Stommel for their comments on the relationship between streamlines and trajectories in the Gulf Stream; B. Owens for the suggestion of using a moving reference frame, T. Rossby, who suggested computing the relative transports, and J. Lillibridge for laying the groundwork of the model in an unpublished manuscript prepared at the University of Rhode Island. This work was completed while the author held a postdoctoral fellowship at the Woods Hole Oceanographic Institution.

REFERENCES

Bower, A. S., and T. Rossby, 1989: Evidence of cross-frontal exchange processes in Gulf Stream meanders based on isopycnal RAFOS float data. *J. Phys. Oceanogr.*, **19,** 1177–1190.

——, H. T. Rossby and J. L. Lillibridge, 1985: The Gulf Stream—barrier or blender? *J. Phys. Oceanogr.*, **15,** 24–32.

——, R. O'Gara and T. Rossby, 1986: RAFOS float pilot studies in the Gulf Stream: 1984–1985. Tech. Rep. Ref. No. 86-7, Graduate School of Oceanography, University of Rhode Island, 110 pp.

Flierl, G., 1981: Particle motions in large-amplitude wave fields. *Geophys. Astrophys. Fluid Dyn.*, **18,** 39–74.

Gilman, Craig S., 1988: A study of the Gulf Stream downstream of Cape Hatteras 1975–1986. MS. thesis, University of Rhode Island, Graduate School of Oceanography, 77 pp.

Halkin, D., and T. Rossby, 1985: The structure and transport of the Gulf Stream at 73°W. *J. Phys. Oceanogr.*, **15,** 1439–1452.

Leaman, K., E. Johns and T. Rossby, 1989: The average distribution of volume transport and potential vorticity with temperature at three sections across the Gulf Stream. *J. Phys. Oceanogr.*, **19,** 36–51.

Owens, W. B., 1984: A synoptic and statistical description of the Gulf Stream and subtropical gyre using SOFAR floats. *J. Phys. Oceanogr.*, **14,** 104–113.

Palmen, E., and C. W. Newton, 1969: *Atmospheric Circulation Systems.* Academic Press, 603 pp.

Regier, L., and H. Stommel, 1979: Float trajectories in simple kinematic flows. *Proc. Nat. Acad. Sci., USA,* **76,** 1760–1764.

Rossby, C.-G., 1942: Kinematic and hydrostatic properties of certain long waves in the westerlies. Misc. Rep., No. 5, Dept. of Meteor., University of Chicago, 37 pp.

Shaw, P.-T., and H. T. Rossby, 1984: Towards a Lagrangian description of the Gulf Stream. *J. Phys. Oceanogr.*, **14,** 528–540.

Watts, D. R., and W. E. Johns, 1982: Gulf Stream meanders: observations on propagation and growth. *J. Geophys. Res.*, **87,** 9467–9476.